Among-species variation in the energy budgets of reef-building corals: scaling from coral polyps to communities

Mia Hoogenboom*[1], Cécile Rottier[2], Severine Sikorski[2], and Christine Ferrier-Pagès[2]

1. *College of Marine and Environmental Sciences and ARC Centre of Excellence for Coral Reef Studies, James Cook University, Townsville, QLD 4811 Australia*
2. *Centre Scientifique de Monaco, 8 Quai Antoine 1er, Monaco MC98000*

* Corresponding author
Phone: +61 (0) 7 4781 5937
Email: mia.hoogenboom1@jcu.edu.au

Submit to: Journal of Experimental Biology
Journal section: Research Article

SUMMARY

The symbiosis between corals and dinoflagellates promotes the rapid growth of corals in shallow tropical oceans, and the high overall productivity of coral reefs. The aim of this study was to quantify and understand variation in carbon acquisition and allocation among coral species. We measured multiple physiological traits (including symbiont density, calcification, photosynthesis and tissue composition) for the same coral fragments to facilitate direct comparisons between species (*Stylophora pistillata*, *Pocillopora damicornis*, *Galaxea fascicularis*, *Turbinaria reniformis* and *Acropora* sp.). Tissue protein content was highly sensitive to the availability of particulate food, increasing in fed colonies of all species. Despite among-species variation in physiology, and consistent effects of feeding on some traits, overall energy allocation to tissue compared with skeleton growth did not depend on food availability. Extrapolating from our results, estimated whole-assemblage carbon uptake varied > 20 fold across different coral assemblages, but this variation was largely driven by differences in the tissue surface area of different colony morphologies, rather than to differences in surface-area specific physiological rates. Our results caution against drawing conclusions about reef productivity based solely on physiological rates measured per unit tissue surface area. Understanding the causes and consequences of among-species variation in physiological energetics provides insight into the mechanisms that underlie in the fluxes of organic matter within reefs, and between reefs and the open ocean.

KEYWORDS: Energy balance, heterotrophic feeding, lipid stores, stable isotope analyses, photosynthesis, scleractinian corals

INTRODUCTION

Nutritional symbioses promote efficient recycling of nutrients in terrestrial, aquatic and marine ecosystems, and involve numerous host and symbiont taxa (Saffo, 1992). One of the most widely recognised nutritional symbioses is that between corals and photosynthetic dinoflagellates from the genus *Symbiodinium* (‘zooxanthellae’). This symbiosis augments the carbon supply to the coral while the symbionts benefit from nutrient supply, and the relatively stable endocellular environment, provided by the coral host (Yellowlees et al., 2008). Additionally, recent studies have revealed nutrient exchange between corals and the microbial community living within the tissue surface layer (Kushmaro and Kramarsky-Winter, 2004; Garren and Azam, 2012) and, also, between corals and endolithic algae colonising the space between coral tissue and skeleton (Fine and Loya, 2002). Overall, coral symbioses are characterised by complex sharing involving nitrogen (Reynaud et al. 2009; Tanaka et al. 2015) and carbon (Hughes et al. 2010; Hughes and Grottoli 2013) that promote the high overall productivity of coral reefs.

In addition to obtaining carbon from symbiont photosynthesis, coral polyps acquire carbon and nutrients through heterotrophic feeding on a variety of sources including zooplankton (e.g. Sebens et al. 1996; Ferrier-Pagès et al., 2003; Palardy et al., 2005), pico- and nano-plankton (Bak et al., 1998; Houlbrèque et al., 2004; Ribes et al. 2003), suspended particulate matter (e.g. Anthony, 1999; Mills et al. 2004) and dissolved organic compounds (e.g., Ferrier, 1991; Grover et al. 2008; Godinot et al. 2011). Early studies on tropical corals suggested that coral reefs were ‘oases’ in the oligotrophic tropical seas and functioned as closed systems with limited exchange of nutrients with the surrounding sea (Odum & Odum 1955; Johannes et al. 1972). However, an alternative view at that time was that heterotrophy provided an important source of nitrogen and phosphorus but contributed little carbon to coral symbioses (Johannes et al., 1970; Muscatine and Porter, 1977). In contrast, recent work

indicates that heterotrophy can actually contribute 70 - 100% of daily carbon requirements (Houlbrèque and Ferrier-Pagès, 2008; Grottoli et al. 2006). Moreover, some coral species up-regulate heterotrophic feeding when photosynthesis is suppressed, either due to decreased light availability (Anthony and Fabricius, 2000; Tremblay et al. 2015), or when symbionts are lost from coral tissue (Palardy et al 2008 and Grottoli et al 2014). Given that heterotrophic feeding can contribute up to 150% of C requirements, understanding how changing environmental conditions are likely to influence the productivity of coral communities requires knowledge of plankton and particulate matter abundance, and of the rates of particulate matter uptake by corals.

Particulate matter and dissolved nutrients can be present at high concentrations in coral reef waters. Although daytime standing stocks of zooplankton can be very low (see Heidelberg et al. 2004), shortly before sunset demersal zooplankton begin to rise into the water column and reach concentrations up to ~10 mg m^{-3} (Yahel et al. 2005; Heidelberg et al. 2004). Moreover, hydrodynamic features like upwellings and internal waves can lead to large increases in plankton densities in shallow waters (Leichter et al. 1998; Roder et al. 2010). Similarly, strong currents can interact with benthic topography to concentrate plankton from a large volume of water into a comparatively small area, greatly amplifying local zooplankton densities (Genin 2004). Even when nutrients are in low concentrations in open waters, the dissipation of energy as waves impinge onto topographically complex reefs drives high dissolved nutrient uptake rates by benthic organisms (Hearn et al. 2001). Finally, in inshore habitats, concentrations of nutrient rich sediments can be up to12 µM NO_3 and 2 M PO_4 (Devlin and Brodie 2005). Collectively, these studies highlight the potential for high local concentrations of nutrient-rich particulate matter in some reef environments.

In addition to variation in particulate matter uptake due to fluctuations in availability in the ocean, the magnitude of particulate carbon uptake by reefs is likely to be influenced by the

species composition of the benthic community. Consistent with this hypothesis, the few studies that have directly quantified the contribution of particulate food to reef ecosystems (i.e., benthic pelagic coupling) have revealed 25-fold variation in uptake rates. Early work in the Caribbean indicated a removal of 34% (by volume) of particulate matter from the water column by benthic reef organisms (Glynn 1973), where baseline levels of particulate matter ranged between 1 – 4 mg **N** m^{-3} (equivalent to ~10 mg m^{-3} of organic matter). Other studies have shown changes in the abundances of different plankton groups between the open water and reef flat which summed to un uptake rate of ~0.1 g C m^{-2} d^{-1} (e.g. Ayukai 1995), and import of carbon from ocean to reef of ~0.2 g C m^{-2} d^{-1} due to the activity of suspension feeding sponges, bivalves and tunicates (Genin et al. 2009). In coral dominated areas, net import of particulate carbon from ocean to reef has been estimated at ~2.5 g C m^{-2} d^{-1} (Fabricius & Domisse 2000). Variation in uptake rates between locations is likely to be partly due to spatial variation in plankton availability; for instance a recent study reported that plankton biomass ranged from 1.0 to 15.6 mg C m^3 on Jamaican reefs (Heidelberg et al. 2004). However, additional research is required to quantify how different assemblages of reef benthic organisms vary in their reliance on externally supplied carbon.

Determining the effect of plankton feeding on coral growth additionally requires knowledge of how heterotrophic carbon is allocated to tissue biomass versus skeletal growth. To date, studies into the role of heterotrophic feeding on coral energetics have revealed species-specific effects. For instance, experimentally starved colonies of *Galaxea fascicularis* had the same lipid content as fed colonies whereas starved *Stylophora pistillata* had approximately 50% lower lipid content than fed colonies (Borell et al. 2008). However, detailed analysis of whether and how heterotrophic feeding influences the energy budgets of different coral species is confounded by differences among published studies in terms of species selection, environmental conditions and measuring techniques. The aims of this study

were to quantify variation in carbon acquisition and allocation among coral species, and in response to food availability, and to determine whether energy allocation to tissue compared with skeletal growth is fixed or plastic in response to changes in food availability. In addition, we aimed to resolve whether and how heterotrophic feeding alters the sharing of carbon and nitrogen between coral host and symbionts by analysing differences in the isotopic composition of symbionts compared with coral tissue. Finally, we extrapolated our results to assess whether and how coral species composition potentially alters the uptake of particulate matter from the water column. We measured multiple physiological traits for the same coral fragments to facilitate direct comparisons within and among species. Understanding the causes and consequences of among-species variation in physiological energetics provides insight into the mechanisms that underlie variation in the fluxes of organic matter within reefs, and between reefs and the open ocean.

MATERIALS AND METHODS

Study species and experimental treatments

Five coral species that are generally abundant on coral reefs were compared: *Stylophora pistillata* (Pocilloporidae), *Pocillopora damicornis* (Pocilloporidae), *Galaxea fascicularis* (Euphylliidae), *Turbinaria reniformis* (Dendrophyllidae) and *Acropora* sp. (Acroporidae) (where family-level taxonomic classification follows Budd et al. [2012]). Six genetically distinct coral colonies per species were originally sourced from the Red Sea and maintained for several months under culture conditions at the Centre Scientifique de Monaco (temperature 26°C ± 0.2°C, light 150 µmol photons m^{-2} s^{-1} using metal halide lights on a 12 h light/dark cycle). Temperature was maintained using thermostat-regulated aquarium heaters (Visy-Therm, 300W). A total of 36 small experimental colonies (nubbins, surface area 5 to 8 cm^2) per species, 6 nubbins from each parent colonies, were created prior to the experiment,

were evenly distributed into 6 glass aquaria (20 L volume) and allowed to recover for 4 weeks. During the recovery period, nubbins were not provided with food in order to remove any previous feeding effect on their physiology (see Shick et al. 2005). During the experimental period (5 weeks), nubbins in three of the six tanks (18 per species) were provided with *Artemia salina* nauplii three times a week (feeding density of approximately 2000 prey per nubbin per feeding event) whereas nubbins in the remaining three tanks (18 per species) received no food at all. After 5 weeks incubation under fed and unfed conditions, the 18 nubbins per treatment and species were divided as follows: 6 nubbins for the feeding rate measurements and the lipid determination; 6 nubbins for measurement of photosynthesis/respiration and symbiont, chlorophyll and protein concentrations; 6 nubbins for the growth rate measurements and the $\partial^{13}C$ and $\partial^{15}N$ isotopic signature of the tissue.

Heterotrophic feeding rates

Nubbins were individually placed in a 2 L volume Plexiglas® flow chamber (Ferrier-Pagès et al. 2010), allowed to acclimate for 30 min until their tentacles were fully expanded, and then incubated in the dark with an initial concentration of ~2000 *Artemia* nauplii per chamber. A control tank without a coral nubbin was also included to account for natural mortality of nauplii during these incubations. Feeding rate was determined from the change in *Artemia* concentration during the incubation, with samples taken from each chamber at the beginning and the end of the incubation and counted using a binocular microscope. Feeding rates were normalized per unit nubbin surface area as determined using the foil-wrapping technique (Marsh 1970).

Photosynthesis and respiration

Rates of photosynthesis and respiration were measured using a set of six temperature-controlled respirometry chambers (50 ml volume) coupled with a Strathkelvin oxygen electrode system (Strathkelvin 928 meter with computer interface). Electrodes were calibrated

using N_2- and air-bubbled seawater as 0% and 100% oxygen saturation values respectively. Respiration was measured during incubation in darkness (30 mins). Subsequently, light intensity was increased stepwise to 150 µmol photons m^{-2} s^{-1} and then 300 µmol photons m^{-2} s^{-1}, and photosynthesis rates were measured at each light level during a 15-minute incubation. Two light levels were used to ensure that photosynthesis had reached saturation (to estimate maximum photosynthesis rates) and feeding and species effects were consistent regardless of which light level was analysed. Rates were normalized to skeletal surface area as determined by foil wrapping (see above).

Skeleton growth and coral tissue and symbiont properties

Nubbins were weighed using the buoyant weight technique (Davies 1989) at the beginning and end of the experiment. From these weights, growth was calculated as the total weight increase over the experimental period and was not normalised to surface area or initial nubbin size. Skeletal micro-density was determined from the difference in dry and water-saturated buoyant weight of skeleton samples of each species after Bucher et al. (1998). Micro-density measurements were subsequently converted to bulk-density assuming porosity of 58% for *Acropora* (Bucher et al. 1998), 60% for *Turbinaria* (based on values for its close relative *Leptopsammia*, Caroselli et al. 2011). Bulk skeletal density estimates for *Pocillopora* and *Stylophora* (1.71 and 1.72 respectively) were from Marshall (2000), and estimated for *Galaxea* based on values for its relative *Gardineroseris* of 1.63 (Manzello 2010).

For chlorophyll and protein concentrations, as well as symbiont density, tissue of each nubbin was removed from the skeleton using an air-pick, and collected in a beaker with 8 ml of 0.45 µm filtered seawater. The tissue slurry was homogenized using a Potter tissue grinder and a 1 ml sub-sample was taken for symbiont counts, which were made using an inverted microscope (Leica, Wetzlar, Germany) and the Histolab 5.2.3 image analysis software (Microvision, Every, France). Five ml of the remaining tissue slurry was centrifuged at 8000

g for 10 min. The supernatant was removed and the symbionts re-suspended in 5 ml of acetone for extraction of chlorophylls *a* and c2 during 24h in darkness. Chlorophyll content was determined using a spectrophotometry method according to Jeffrey and Humphrey (1975). The remaining slurry was incubated in sodium hydroxide (0.5 N) maintained in a water-bath for 30 minutes at 90°C for protein determination. Briefly, concentrations were estimated using a bicinchoninic acid protein assay (Uptima, Interchim) by reference to standards across a concentration range from 0 to 2000 μg ml^{-1} that were prepared using Bovine Serum Albumin (BSA, Interchim). Absorbance was measured at 560 nm, and sample protein content was determined using GENESIS (Kontron Instruments), and was normalized to the skeletal surface area.

Lipid content was quantified according to Hoogenboom et al. (2010), using a modification of the method developed by Bligh and Dyer (1959). Briefly, frozen nubbins were ground into a fine powder using a mortar and pestle and mixed with a solution of dichloromethane, methanol and distilled water. Samples were sonicated for 10 min, incubated at 40°C for 1 h and filtered through Whatman GF/C filters to remove skeleton fragments from solution. Subsequently, 1.5 ml of both dichloromethane and methanol were added to the filtrate and the solution centrifuged at 2000 rpm for 10 min to separate the phases. The lower lipid containing-layer was transferred into cleaned, pre-combusted and pre-weighed glass vials (4 ml). The solution was evaporated under nitrogen, and the amount of lipid determined by weight.

Carbon and nitrogen isotopic determination

Carbon and nitrogen isotopic determination was performed in each component of the symbiotic association (symbionts and host) to trace how nutrients are shared within the symbiosis. We expected that heterotrophic feeding would change the isotopic composition of the host tissue more than the symbionts since particulate nutrients are first ingested and

digested by the coral host. Nubbins were individually placed in 100 mL beakers, containing 20 ml of filtered seawater, which had been pre-combusted at 480°C for at least 4 h in a ThermolyneH 62700 oven. Tissue was completely removed from the skeleton with an air pick and homogenized with a Potter tissue grinder. The homogenate was separated into host and symbiont fractions by centrifugation at 3000 g for 10 min to pellet the symbionts (at 4°C). Centrifugation of the supernatant was repeated twice in order to entirely remove any remaining symbionts, and the supernatant was subsequently flash frozen in liquid nitrogen, and freeze-dried using a Heto (model CT 60) drier. For the symbiont fraction, the pellet was washed several times with filtered seawater (to remove any residual host tissue) before being flash frozen and freeze-dried as above. Samples were analyzed for $\delta^{15}N$ and $\delta^{13}C$ using a Geo-20:20 isotope ratio mass spectrometer (SerConH). Scale calibration of results was performed using international reference materials (IAEA-600 and IAEA-CH6, International Atomic Energy Agency) and two control samples were analyzed with each batch for quality control purposes. Precision, as determined by repeat analysis of controls and reference materials, was better than ± 0.20% and ± 0.15% for measured $\delta^{15}N$ and $\delta^{13}C$ values, respectively.

Data Analysis

Values reported in the text as given as means ± standard error. Two-way mixed-effects analysis of variance (ANOVA) was used to determine whether provision of food affected coral energy acquisition and allocation, with species and feeding regime treated as fixed factors and ‘tank’ was included as a random effect. Raw data were square root or log transformed so that the data were appropriate for ANOVA, as assessed by visual inspection of normal QQ plots and plots of residuals versus fitted values. Stable isotope data were analysed using general linear mixed effects models to account for the repeated measure of different tissues (i.e., symbiont tissue and host tissue) sampled from the same coral fragment. In this analysis, coral fragment identity was treated as a random factor and the error term of the

mixed-effects model specified that tissue type was nested within fragment. For all analyses, minimal models are presented with non-significant terms removed using a backwards deletion procedure. Analyses were implemented in R (version 2.14.1, The R Foundation for Statistical Computing Team 2011) using the function 'lme' in the package 'nlme'.

The contribution of heterotrophic feeding to animal respiration (i.e., CHAR, after Grottoli et al. 2006) was calculated by multiplying feeding rate (measured as nauplii cm^{-2} h^{-1}) by the carbon content of nauplii (0.68 µg C $nauplii^{-1}$, Wijgerde et al. 2011) by the duration of the feeding period (2 h) and then dividing this rate by the measured respiration rate converted to carbon equivalents with values normalised to tissue surface area (as per Hoogenboom et al. 2010). Energy allocation to skeleton growth was calculated from the measured total calcification across the experiment (g) multiplied by the energy cost of calcification (0.152 J mg^{-1}, Anthony et al. 2002). Differences in energy allocation to tissue versus skeletal growth were determined by first converting the measured calcification per coral fragment (change in buoyant weight, g) into a change in colony volume (cm^3) given the density of the calcium carbonate skeleton (where increase in colony volume [cm^3] = production of new skeleton [g] divided by skeletal density [g cm^{-3}]). Subsequently, we calculated the increase in surface area that corresponded to the calculated increase in colony volume based on coral nubbin morphology. To do so, we represented fragments as cylinders with a 'branch' radius of 6 mm for *Stylophora* and *Pocillopora* and 4 mm for *Acropora*, or as plates with a height of 5 mm for *Turbinaria* and 10 mm for *Galaxea*. Geometric formulae for the surface area and volume of a cylinder were used to calculate the change in tissue surface area corresponding to the measured change in volume. Energy allocation to tissue was then estimated from the calculated change in tissue surface area multiplied by the measured lipid and protein content per unit surface area (converted to energy equivalents of 23.9 J mg^{-1} for protein and 39.5 J mg^{-1} for lipid, Gnaiger & Bitterlich 1984). We did not account for carbohydrates because they

typically contribute less than 10% of coral tissues (Leuzinger et al. 2003). Finally, given that these calculations depend on several parameters that are estimated with error, we conducted a sensitivity analysis to assess how variation in parameter values influenced proportional energy allocation to tissue (see Supplementary Material).

Carbon acquisition of simulated coral assemblages

Total carbon uptake (from net photosynthesis and heterotrophic feeding) was simulated for different coral assemblages composed of different combinations of the study species. We use the measured data (photosynthesis, respiration, heterotrophic feeding, lipid content and protein content), and scaled up from measurements per unit tissue surface to values per m^2 of reef taking to account the surface area to horizontal planar area ratios of the different genera. For the (flat) laminar/encrusting morphologies (*Galaxea* and *Turbinaria*) colony tissue surface area is equivalent to horizontal planar area. For the branching morphologies, colony tissue surface area was calculated based on measured branch densities (branches cm^{-2}) for *Acropora valida* (as a proxy for *Acropora* sp. used herein) and *Pocillopora damicornis* (as a proxy for *Pocillopora* and *Stylophora* used herein). These branch density estimates were determined from field photographs of *A. valida* and *P. damicornis* from Lizard Island (northern Great Barrier Reef) and Orpheus Island (central Great Barrier Reef). All photographs were taken from directly above coral colonies and included a ruler as a scale bar and were analysed using ImageJ. Branch surface area (based on branch diameter) was calculated for each genus then multiplied by branch density to obtain tissue surface area per unit reef occupied (i.e., horizontal planar area). To account for effects of morphological variation within species (e.g., *Turbinaria* colonies range from encrusting to cone-shaped with multiple tiers) we repeated the calculations for different colony shapes. Moreover, previous studies indicate that different proportions of the coral tissue surface actively capture particles from the water column, ranging from branch tips (Palardy et al., 2005) to branch bases at the

centre of colonies where plankton can become trapped in interstitial spaces (Schiller & Herndl 1989). To account for this, we repeated calculations for branching assemblages allowing active particle feeding for different proportions of the total colony surface area. For each simulated coral assemblage we calculated total carbon uptake (g C m^{-2} d^{-1}, with daily respiration subtracted from daily photosynthesis and converted to carbon equivalents as above), particulate carbon uptake (g C m^{-2} d^{-1}, calculated based on feeding rates and an estimated carbon content of plankton of 0.68 µg C $plankton^{-1}$; see above) and total coral tissue biomass (g m^{-2}, calculated as the sum of protein and lipid content per unit surface area multiplied by colony tissue surface area). We note that these calculations assume that area-specific rates are independent of colony diameter and are intended to identify relative variation among the assemblages rather than to predict absolute rates of carbon uptake under field conditions.

RESULTS

Among-species variation in symbiont properties and carbon acquisition

The effect of feeding on the density of symbionts within coral tissue varied among the study species (Table 1). Provision of food enhanced symbiont density for *Acropora*, *Pocillopora* and *Stylophora* but not for *Galaxea* or *Turbinaria* (Fig 1A). Among the five species, *Stylophora* had the highest average symbiont density but values for this species were similar to those of *Turbinaria* and *Galaxea* (Tukey's HSD, $p > 0.75$ for both comparisons) while densities for *Acropora* and *Pocillopora* were 2 – 3 fold lower (Fig 1A). Variation in total chlorophyll concentration (Chl a $+c_2$) in response to feeding was generally consistent with observed variation in symbiont densities for *Acropora, Pocillopora* and *Turbinaria* (Fig 1B), although this difference was not significant for *Pocillopora* (post-hoc test, $p = 0.07$). However, fed nubbins of *Stylophora* did not have higher chlorophyll content than unfed

nubbins despite the increase in symbiont population density with feeding, reflecting a decrease in chlorophyll per symbiont cell for fed nubbins (data not plotted). Conversely, chlorophyll content was significantly higher in fed nubbins of *Turbinaria* although feeding did not significantly enhance symbiont numbers for this species.

Neither rates of photosynthesis nor dark respiration varied significantly with food availability for any of the study species (Table 1), despite a general trend toward increased photosynthesis rates in fed nubbins of all species except for *Turbinaria* (Fig 1C). Measured rates of dark respiration (Fig 1D) were approximately equivalent for all species except for *Acropora*, for which rates where ~3-fold lower, and were not influenced by food availability (Table 1, Fig 1D). Grazing rates of coral nubbins on *Artemia salina* nauplii ranged between 9.6 ± 3.6 to 188 ± 15.9 nauplii cm^{-2} h^{-1} for *Acropora* and *Pocillopora* respectively, with the other species intermediate in this range (Table 2). The ratio of photosynthesis to respiration, converted to units of μg C cm^{-2} d^{-1}, ranged from 1.06 ± 0.14 for *Pocillopora* to 1.41 ± 0.08 for *Galaxea* with the other species intermediate within this range (Table 2). The contribution of total acquired carbon to animal respiration (CTAR, calculated as the sum of daily photosynthetic plus heterotrophic carbon acquisition relative to daily respiration) was > 100% for all species (Table 2) with *Pocillopora* > *Stylophora* > *Acropora* > *Galaxea* > *Turbinaria*.

Among species variation in calcification and tissue composition

Skeleton growth over the total duration of the experimental period ranged from 0.14 to 3.8 g and was highest for *Turbinaria* and *Stylophora* which showed approximately equivalent growth of 2.3 ± 0.27 and 1.7 ± 0.16 g respectively compared with ~0.50 to 0.75 g for the other species. Skeleton growth was generally higher for fed compared with unfed nubbins overall but this effect was not statistically significant (Table 1, Fig 2A), nor did it depend on species identity (ANOVA, species by feeding interaction term, $F_{4,50} = 1.5$, $p = 0.21$). Skeletal micro-density was not influenced by food availability (Table 1, Fig 2D), but *Galaxea* had

higher skeletal density than all other species (post-hoc test, pairwise comparisons between *Galaxea* and other species, $p < 0.03$ in all cases). *Pocillopora* and *Turbinaria* had the lowest skeletal density, although density of *Turbinaria* was not significantly different than *Stylophora* and *Acropora* which had intermediate density (Fig 2D).

Tissue composition varied among species and in response to feeding. Protein content was highest, on average, for nubbins of *Turbinaria* (1.9 ± 0.12 mg cm^{-2}) followed by *Galaxea* (1.2 ± 0.07 mg cm^{-2}) and levels for these species were significantly different from each other and from those of the three branching species (Tukey's HSD, $p < 0.01$ for all comparisons). As observed for skeletal growth rates, protein levels were higher in fed compared with unfed nubbins overall (Table 1, Table 3) independently of species identity (ANOVA, species by feeding interaction term, $F_{4,50} = 1.3$, $p = 0.30$, Figure 2B). In contrast to the consistent effect of feeding on tissue protein, lipid concentrations were only significantly higher in fed compared with unfed nubbins of *Pocillopora* and *Turbinaria* (Figure 2C). On average, *Stylophora* had the highest lipid content (1.3 ± 0.09 mg cm^{-2}), *Pocillopora* had the lowest lipid content (0.56 ± 0.09 mg cm^{-2}) and the other three species were intermediate between these levels.

Symbiont and host tissue isotopic ratios

$\delta^{15}N$ isotopic values ranged from ~3.3 - 8.3‰ overall, but comparison of the effects of tissue type (host versus symbont) and food availability (fed versus unfed) could only be conducted for three species due to missing data for symbionts within unfed nubbins of *Acropora* and *Pocillopora.* This analysis revealed that fed corals (overall, pooled across species and tissue types), tended to have higher $\delta^{15}N$ (Feeding main effect, Table 1) than unfed corals. However, host and symbiont tissues only differed in $\delta^{15}N$ for *Stylophora,* (Fig 3A, post-hoc test, host versus symbiont comparison, $p = 0.17$ and 0.35 for *Galaxea* and *Turbinaria* respectively). When only the fed nubbins of all species were compared in a

separate analysis, symbiont $\delta^{15}N$ values were higher than host tissue for *Stylophora* (post-hoc test, host versus symbiont comparison, $p < 0.02$), lower than host tissue for *Pocillopora* (post-hoc test, host versus symbiont comparison, $p < 0.001$) but equivalent to host tissue for the remaining three species (Fig 3A, post-hoc test, host versus symbiont comparison, $p > 0.27$ in all cases). $\delta^{13}C$ isotopic ratio ranged from ~-29 ‰ to ~-11‰ and was more positive in symbiont compared with host tissue for *Acropora*, *Galaxea* and *Pocillopora* (Table 1, Fig 3B). In addition, $\delta^{13}C$ isotopic ratio was higher in unfed compared with fed nubbins for *Acropora* (but not for the other four species; Table 3, Fig 3B).

Relationships between physiological traits and relative heterotrophic feeding rates

The high variation in feeding rates corresponded to CHAR values between 14% (± 1%) to 159% (± 39%) for *Galaxea* and *Pocillopora* respectively with the other three species intermediate within this range (Fig 4). Feeding rates were more variable between species than photosynthesis rates and this meant that the rank order of species based on the ratio of total carbon acquisition to coral respiration was generally similar to the rank order of species based on CHAR, with *Pocillopora* and *Stylophora* having considerably higher values than the other three species. Based on simple geometric relationships between surface area and volume of coral branches (*Acropora*, *Pocillopora*, *Stylophora*) and plates (*Turbinaria*, *Galaxea*), the proportion of energy allocated to tissue biomass (relative to skeletal growth) ranged from 31% to 74% overall (absolute range across all nubbins). There was no evidence that allocation to tissue was higher in fed compared with unfed nubbins (data not plotted, two-way ANOVA, feeding effect on energy allocation, $F_{1,50}=2.3$, $p = 0.14$). However, allocation did vary among species (Figure 4A, two-way ANOVA, species effect on energy allocation, $F_{4,50}=11.3$, $p < 0.001$). Energy allocation was similar for *Stylophora*, *Pocillopora* and *Turbinaria* (Tukey's post-hoc test, $p > 0.58$ for all relevant pairwise comparisons) and values for these three

species were lower than values for *Galaxea* and *Acropora* (Tukey's post-hoc test, $p < 0.02$ for all relevant pairwise comparisons).

Energy allocated to tissue versus skeleton was higher in species that had a lower reliance on heterotrophic feeding (Fig 4A, Pearson's correlation between CHAR and energy allocation to tissue, arcsin transformed proportion data, $r=-0.49$, $t_{28}=-3.04$, $p < 0.01$). Note that only data for fed nubbins was analysed because CHAR = 0 for the unfed nubbins in our experiment. In contrast, there was not an obvious trend in the relationships between CHAR with the differences in $\delta^{13}C$ and $\delta^{15}N$ between host versus symbiont tissue from the same fragments (denoted by $\Delta\delta^{13}C$ and $\Delta\delta^{15}N$ respectively hereafter) because the values for *Pocillopora* were not consistent with the trend observed for the other four species. For the carbon isotopic ratio, the largest differences in host and symbiont values occurred when CHAR was very low (<30%) or very high (>150%). For nitrogen, differences between host and symbiont values occurred when CHAR was >100% but this difference was positive for *Stylophora* and negative for *Pocillopora*.

Differences in $\Delta\delta^{13}C$ between host and symbiont tissues were generally consistent with differences in $\Delta\delta^{15}N$ between host and symbiont, except for *Pocillopora* (Fig 4B and C). When data from both fed and unfed colonies were included there was a general trend toward a larger $\Delta\delta^{13}C$ associated with increased $\Delta\delta^{15}N$ (Fig 5). However, this relationship was not statistically significant (Pearson's correlation, $R = -0.38$, $t_{19}=-1.8$, $p =0.09$) as there was high variation in $\Delta\delta^{15}N$ for colonies for which $\Delta\delta^{13}C$ values were small. In addition, there were two colonies that showed values inconsistent with the general trend (two *Acropora* with $\Delta\delta^{13}C > 8$ but $\Delta\delta^{15}N \sim 1$). In contrast, the magnitude of the difference between host and symbiont values was correlated with symbiont density within coral tissue for $\delta^{15}N$ (Fig 6B, Pearson's correlation, $R = -0.77$, $t_6=-2.9$, $p < 0.03$) with a similar, but not statistically

significant, association observed for $\delta^{13}C$ (Fig 6A, Pearson's correlation, R = -0.53, t_8=-1.8, p =0.12).

Carbon acquisition of simulated coral assemblages

Net carbon uptake of simulated coral assemblages varied >20-fold depending on species composition (Table 4). The assemblage composed of only encrusting/laminar colony morphologies (i.e., *Galaxea* and *Turbinaria*) had the lowest total carbon uptake (~0.76 g C m^{-2} d^{-1}) despite the relatively high gross photosynthesis rates of these genera (Figure 1). In contrast, the assemblage composed of the three branching genera (i.e., *Acropora*, *Stylophora* and *Pocillopora*) had substantially higher total carbon uptake (~12.1 g C m^{-2} d^{-1}) and higher particulate carbon uptake (~9.6 g C m^{-2} d^{-1}). These differences were primarily driven by the much higher surface area to horizontal planar area ratio of branching compared with other morphologies (as indicated by the higher total tissue biomass of these assemblages, Table 4). Morphological plasticity, such as changes in colony shape observed for *Turbinaria* along a light intensity gradient, had a relatively small influence on particulate and total carbon uptake by coral assemblages (Table 4). In contrast, for branching species, decreasing the proportion of the tissue surface actively involved in particle capture substantially decreased whole-assemblage uptake of particulate carbon (Table 4). However, uptake by the assemblage of branching species remained higher than that of the non-branching species as long as the area of the effective feeding surface was > 6% of the total tissue surface area.

DISCUSSION

Of the 9 physiological traits measured in this study, tissue protein content was the most sensitive to the availability of particulate food, increasing in fed colonies of all five study species (as summarised in Table 3). Symbiont density and chlorophyll content were influenced by food availability only for certain species, whereas whole-colony photosynthesis

and respiration rates were independent of feeding for all species. Despite among-species variation in physiology, and consistent effects of feeding on some traits, overall energy allocation to tissue compared with skeleton growth did not depend on feeding status, primarily because both calcification and tissue quality (protein content) were enhanced by feeding (although the effect of feeding on calcification was not statistically significant). δ^{15}N was a reliable indicator of heterotrophic feeding because it was higher in tissues of fed *Galaxea* and *Turbinaria*, significantly different between symbiont and host for *Stylophora* and *Pocillopora* (data available for fed corals only) and the difference in δ^{15}N between host and symbiont decreased with increasing symbiont density. Finally, estimated whole-community carbon uptake varied > 20 fold across different simulated coral assemblages. However, this variation was driven by differences in the tissue surface area to horizontal planar area ratio for different colony morphologies, and by differences in the effective feeding surface area of branching morphologies. Clearly, accurately quantifying the size of the effective feeding surface area is important for accurate prediction of particulate matter uptake by coral assemblages.

Nutrient sharing between coral host and symbionts

Stable isotopes are increasingly used in dietary and food web studies (Petersen and Fry, 1987) and are a valuable technique for tracking the exchange of nutrients within symbiotic associations (e.g., for Hughes et al. 2010; Tremblay et al., 2014). To date, several studies of coral feeding ecology have quantified the difference between symbiont and coral host isotopic ratios, with larger differences implying a greater reliance on heterotrophy. Such inferences are supported by the general trend of increased differentiation between host and symbiont isotope ratios as depth and heterotrophy increase to compensate for the decrease in light and photosynthetic productivity (Land et al., 1975; Muscatine and Kaplan 1994; Lesser

et al., 2010). In natural field settings, coral symbiont density, or the chlorophyll content of symbionts, tends to increase with depth to maximise light interception (Porter et al.1984; Titlyanov et al. 2001; Frade et al. 2008). In this study we observed that host and symbiont isotopic composition were more similar in corals with high symbiont densities suggesting that increased translocation of nutrients from coral host to symbiont (e.g., due to increased particulate feeding by the host) may drive an increase in symbiont density and a corresponding similarity in host and symbiont isotopic composition.

Our results suggest that nitrogen is exchanged and shared differently between coral host and symbionts compared with carbon: carbon isotopic composition was significantly different between coral and symbiont tissues for *Acropora*, *Galaxea* and *Pocillopora* whereas nitrogen isotopic composition was significantly different between coral and symbiont tissues for *Stylophora* and *Pocillopora*. Although further studies on a greater number of species are required, our study suggests that differences between symbiont and host are associated with CHAR; variation in $\delta^{13}C$ values occurred only when CHAR was very low or very high and variation in $\delta^{15}N$ was only observed in species for which CHAR was above 70%. Differentiation between host and symbiont when CHAR is high is consistent with the broader literature. However, differentiation in host and symbiont $\delta^{13}C$ for *Acropora* and *Galaxea*, species that had low CHAR values indicates that $\delta^{15}N$ may be a more reliable indicator of coral heterotrophic feeding than $\delta^{13}C$. Nevertheless, carbon translocation from symbiont to host can vary with particle feeding rates (Hughes et al. 2010; Tremblay et al., 2014) and a decrease in the amount of carbon translocated to the host when feeding rates are low and nutrient supply is limited, could drive differentiation in host and symbiont $\delta^{13}C$. Finally, we note that the $\delta^{13}C$ values for symbiont and host observed here are more negative compared with other studies (e.g., -11‰ to -14‰ in Nahon et al. 2013; or -13‰ and -16‰ in Swart 1983). Likely explanations for this observation include the relatively low light levels under

which corals were grown in our study: several studies have found decreasing $\delta^{13}C$ with depth (e.g., Grottoli and Wellington 1999; Alamaru et al., 2009; Lesser et al. 2010). In addition, these values are likely to depend upon the nutritional value of the food source and the observed $\delta^{13}C$ signal may reflect that of the *Artemia* used in our study (-29‰, 1.24 ± 0.5 μg C nauplii^{-1} and 0.25 ± 0.01 μg N nauplii^{-1}.).

Energy allocation between tissue and skeleton

Results of this study indicate that resource (i.e., energy and nutrients) allocation between tissue and skeleton growth is not sensitive to changes in plankton availability. Most energy budget models allow for variation in energy allocation between growth, reproduction and basic maintenance across an individual's lifespan, depending on body size and food availability (e.g., MacCauley et al., 1990). Similarly, over evolutionary time scales, selection can drive variation in energy allocation; for instance, among-species variation in energy allocation to reproduction in fishes is related to population-specific adult mortality rates (Lester et al., 2004). Research on corals indicates that tissue growth precedes skeletal growth, with corals increasing their tissue before new skeleton is produced (e.g., Ferrier-Pages et al. 2003; Houlbreque et al. 2004) which could lead to a tight coupling between tissue and skeleton growth that would constrain variation in relative energy allocation. More broadly, a fixed energy allocation pattern indicates that changes in particulate food availability are likely to cause a general decline in coral growth rather than a change in energy allocation occurring that maintains skeleton growth and the expense of tissue growth (or vice versa).

Scaling from coral polyps to communities

Our results demonstrate that there is high among-species variation in carbon uptake, and indicate that the fluxes of carbon into and out of coral assemblages are likely to vary in

response to changes in species composition. While we acknowledge the limitations of extrapolating results from laboratory experiments to natural field environments, this study indicates that coral communities dominated by branching morphologies (with a high coral tissue surface area to planar area ratio) potentially uptake a much greater amount of particulate and photosynthetic carbon, although their uptake of particulate carbon depends on the proportion of the tissue surface that encounters and captures prey. Branching corals also excrete 40 – 60% of acquired carbon (Crossland et al., 1980; Davies 1984), and hence, carbon fluxes from reefs dominated by branching species are likely to exceed those of other coral assemblages. Although few studies have systematically compared the total productivity of different coral assemblages, evidence in the literature supports the interpretation of greater carbon flux from assemblages dominated by branching corals. For example, *Acropora*-dominated communities produce 15.3 to 16.6 g C m^{-2} d^{-1} (Gattuso et al., 1996 and Smith 1981, respectively) compared with 1.3 to 9.9 g C cm^{-2} d^{-1} for mixed benthic assemblages of corals, macroalgae and crustose corallite algae (Atkinson & Grigg 1984; Bates 2002; Gattuso et al., 1996).

Consistent with studies of coral heterotrophy conducted over the past decade (e.g., Houlbreque et al. 2004; Grottoli et al., 2006; 2014) our results demonstrate that particle feeding contributes substantially to the energy budgets of certain coral species, with CHAR values ranging between 14% (for *Galaxea*) to 150% (for *Pocillopora*). Moreover, CHAR is typically calculated based on macroplankton and is likely to be higher if all possible heterotrophic feeding sources are considered (e.g., Tremblay et al. 2011). This is of concern because the species composition and body size distribution of plankton are regulated by physical and chemical conditions (Richardson 2008) and are likely to change under climate change conditions. Presently, there is limited direct evidence of spatial variation in the extent to which different coral reefs, and/or different assemblages of coral species, consume

plankton and other particulate matter. However, studies using stable isotope techniques have shown that corals in deeper waters consume more plankton than corals in shallow habitats (Muscatine et al. 1989; Grottoli 1999; Alamaru et al 2009). Similarly, there is evidence of among-reef variation in the carbon and nitrogen isotopic composition of coral tissues (Heikoop et al. 2000), and a recent study has demonstrated that spatial variation in coral tissue composition was associated with variation in turbidity (Nahon et al., 2013). Nevertheless, it remains unclear whether such variation in tissue composition is due to corals in different areas consuming different amounts or types of particulate food, or whether corals in different areas have differential reliance on photosynthesis versus particulate feeding. High variation in feeding rates among coral species, and in CHAR and the effects of feeding on coral physiology (this study, Sebens et al. 1996; Ferrier-Pages et al. 2011; Palardy et al. 2005), indicates that predicted changes to plankton communities, and nutrient and sediment run-off, under climate change scenarios (e.g., McKinnon et al 2007; Richardson 2008) may affect the relative abundances of coral species on reefs.

Understanding the causes and consequences of among-species variation in physiological energetics provides insight into the mechanisms that underlie changes in the fluxes of organic matter within reefs, and between reefs and the open ocean. In this study we measured multiple physiological traits for the same coral fragments to facilitate direct comparisons within and among species. Results show that tissue protein content is consistently higher when particulate food is available for corals in general, whereas effects of feeding on symbiont density and chlorophyll content were species-specific. Our findings suggest that energy allocation between tissue and skeletal growth is not sensitive to variation in food availability. Finally, estimated whole-community carbon uptake varied > 20 fold across different simulated coral assemblages and, therefore, our results caution against drawing conclusions about reef productivity based solely on physiological rates measured per

unit tissue surface area without accounting for differences in total tissue surface area among different colony morphologies. Overall these findings indicate that the fluxes of carbon into and out of coral assemblages are likely to vary in response to changes in species composition.

ACKNOWLEDGEMENTS

This research was funded by the Government of the Principality of Monaco through the Centre Scientifique de Monaco (CR, CFP), and James Cook University (MH).

LITERATURE CITED

Alamaru, A., Loya, Y., Brokovich, E., Yam, R., and Shemesh, A. (2009). Carbon and nitrogen utilization in two species of Red Sea corals along a depth gradient: Insights from stable isotope analysis of total organic material and lipids. *Geochim. Cosmochim. Acta,* **73**, 5333-5342.

Anthony, K. R. N. (1999). Coral suspension feeding on fine particulate matter. *J. Exp. Mar. Biol. Ecol.*, **232**, 85–106.

Anthony, K. R. N. and Fabricius, K. E. (2000). Shifting roles of heterotrophy and autotrophy in coral energy budgets at variable turbidity. *J. Exp. Mar. Biol. Ecol.*, **252**, 221–253.

Anthony, K. R. N., Connolly, S.R., & Willis, B.L. (2002) Comparative analysis of energy allocation to tissue and skeletal growth in corals. *Limnol. & Oceanogr*., **47**, 1417–1429.

Atkinson, M. J., and Grigg, R. W. (1984) Model of a coral reef ecosystem II. Gross and net benthic primary production at French Frigate Shoals, Hawaii. *Coral Reefs*, **3**, 3-22

Ayukai, T. (1995). Retention of phytoplankton and planktonic microbes on coral reefs within the Great Barrier Reef, Australia. *Coral Reefs*, **14**, 141-147.

Bak, R. P. M., Joenje, M., de Jong, I., Lambrechts, D. Y. M. and Nieuwland, G. (1998). Bacterial suspension feeding by coral reef benthic organisms. *Mar. Ecol. Prog. Ser.*, **175**, 285–288.

Bates, N. R. (2002) Seasonal variability of the effect of coral reefs on seawater CO_2 and air-sea CO_2 exchange. *Limnol. Oceanogr.*, **47**, 43-52.

Bligh, E. G. and Dyer, W. J. (1959). A rapid method of total lipid extraction and purification. *Can. J. Biochem. Physiol.*, **37**, 911–917.

Borell, E.M., Yuliantri, A.R., Bischof, K. and Richter, C. (2008) The effect of heterotrophy on photosynthesis and tissue composition of two scleractinian corals under elevated temperature. *J. Exp. Mar. Biol. Ecol.* **364**, 116-123.

Bucher, D.J., Harriott, V.J., and Roberts, L.G. (1998) Skeletal micro-density, porosity and bulk density of acroporid corals. *J. Exp. Mar. Biol. Ecol.* **228**, 117-136.

Budd, A.F., Fukami, H., Smith, N.D. and Knowlton, N. (2012) Taxonomic classification of the reef coral family Mussidae (Cnidaria: Anthozoa: Scleractinia). *Zool. J. Linn. Soc.*, **166,** 465-529.

Caroselli, E., Prada, F., Pasquini, L., Marzano, F., Zaccanti, F., Falini, G., Levy, O., Dubsinsky, Z. And Goffredo, S. (2011) Environmental implications of skeletal micro-density and porosity variation in two scleractinian corals. *Zoology*, **114**, 255–264.

Crossland, C. J., Barnes, D. J. and Borowitzka, M. A. (1980). Diurnal lipid and mucus production in the staghorn coral *Acropora acuminata. Mar. Biol.*, **60**, 81-90.

Davies, P. S. (1984). The role of zooxanthellae in the nutritional energy requirements of *Pocillopora eydouxi*. *Coral Reefs* **2**, 181–186.

Davies, P.S. (1989). Short-term growth measurements of corals using an accurate buoyant weighing technique. *Mar. Biol.* **2**, 181–186.

Devlin, M.J., and Brodie, J. (2005). Terrestrial discharge into the Great Barrier Reef Lagoon: nutrient behavior in coastal waters. *Mar. Poll. Bull.*, **51**, 9-22.

Douglas, A.E. (1998). Nutritional interactions in insect-microbial symbioses: aphids and their symbiotic bacteria *Buchnera*. *Annu. Rev. Entomol.* **43**, 17–37.

Fabricius, K.E., and Dommisse, M. (2000) Depletion of suspended particulate matter over coastal reef communities dominated by zooxanthellate soft corals. *Mar. Ecol. Prog. Ser.*, **196**, 157–167.

Ferrier, M. D. (1991). Net uptake of dissolved free amino acids by four scleractinian corals. *Coral Reefs*, **10**, 183–187.

Ferrier-Pagès, C., Witting, J., Tambutté, E. and Sebens, K. P. (2003). Effect of natural zooplankton feeding on the tissue and skeletal growth of the scleractinian coral *Stylophora pistillata*. *Coral Reefs* **22**, 229–240.

Ferrier-Pagès, C., Hoogenboom, M. and Houlbreque, F. (2011) The role of plankton in coral trophodynamics. In Z. Dubinsky and N. Stambler (eds.). Coral Reefs: An Ecosystem in transition. Springer, pp 215 – 229.

Fine, M., & Loya, Y. (2002). Endolithic algae: an alternative source of photoassimilates during coral bleaching. *Proc. Roy. Soc. London B*, **269**, 1205-1210.

Frade, P. R., Bongaerts, P., Winkelhagen, A. J. S., Tonk, L., & Bak, R. P. M. (2008). *In situ* photobiology of corals over large depth ranges: A multivariate analysis on the roles of environment, host, and algal symbiont. *Limnol. Oceanogr.*, **53**, 2711-2723.

Garren, M., & Azam, F. (2012). New directions in coral reef microbial ecology. *Environ. Microbiol.*, **14**, 833-844.

Gattuso, J.-P., Pichon, Delasalle, B., Canon, C., Frankignoulle, M. (1996) Carbon fluxes in coral reefs. I. Lagrangian measurement of community metabolism and resulting air-sea CO_2 disequilibrium. *Mar. Ecol. Prog. Ser.,* **145**, 109-121.

Genin A (2004) Bio-physical coupling in the formation of zooplankton and fish aggregations over abrupt topographies. *J. Mar. Syst.* **50**, 3–20.

Genin, A., Monismith, S. G., Reidenbach, M.A., Yahel, G. and Koseff, J. R. (2009) Intense bentic grazing of phytoplankton in a coral reef. *Limnol. Oceanogr.,* 54(3): 938-951.

Glynn, P. (1973) Ecology of a Carribean coral reef. The *Porites* reef-flat biotope: Part II. Plankton community with evidence for depletion. *Mar. Biol.*, **22**, 1-21.

Gnaiger, E., & Bitterlich, G. (1984). Proximate biochemical composition and caloric content calculated from elemental CHN analysis: a stoichiometric concept. *Oecologia*, **62**, 289–298.

Godinot, C., Houlbreque, F., Grover R, Ferrier-Page`s C (2011) Coral uptake of inorganic phosphorus and nitrogen negatively affected by simultaneous changes in temperature and pH. *PLoS ONE*, **6**, e25024.

Grottoli, A. G., Rodrigues, L. J., Palardy, J. E. (2006). Heterotrophic plasticity and resilience in bleached corals. *Nature,* **440**, 1186–1189.

Grottoli, A. G., Warner, M. E., Levas, S. J., Aschaffenburg, M. D., Schoepf, V., McGinley, M., & Matsui, Y. (2014). The cumulative impact of annual coral bleaching can turn some coral species winners into losers. *Glob. Change Biol.*, **20**, 3823-3833.

Grover, R., Maguer, J. F., Allemand, D., & Ferrier-Pagès, C. (2008). Uptake of dissolved free amino acids by the scleractinian coral Stylophora pistillata. *J. Exp. Biol.*, **211**, 860-865.

Hearn, C., Atkinson, M., & Falter, J. (2001). A physical derivation of nutrient-uptake rates in coral reefs: effects of roughness and waves. *Coral Reefs*, **20**, 347-356.

Heidelberg, K. B., Sebens, K. P. and Purcell, J.E., (2004) Composition and sources of near reef zooplankton on a Jamaican forereef along with implications for coral feeding. *Coral Reefs*, **23**, 263-276.

Heikoop, J. M., Dunn, J. J., Risk, M. J., Tomascik, T., Schwarcz, H. P., Sandeman, I. M., and Sammarco, P. W. (2000) $\delta^{15}N$ and $\delta^{13}C$ of coral tissue show significant inter-reefal variation. *Coral Reefs*, **19**, 189-193.

Hoogenboom, M.O., Rodolfo-Metalpa, R., and Ferrier-Pages, C. (2010) Co-variation between autotrophy and heterotrophy in the Mediterranean coral *Cladocora caespitosa*. *J. Exp. Biol.*, **213**, 2399–2409.

Houlbrèque, F. and Ferrier-Pagès, C. (2008). Heterotrophy in tropical scleractinian corals. *Biol. Rev.*, **84**, 1-17.

Houlbrèque, F., Tambutté, E., Richard, C. and Ferrier-Pagès, C. (2004). Importance of a micro-diet for scleractinian corals. *Mar. Ecol. Prog. Ser.*, **282**, 151–160.

Hughes, A. D., Grottoli, A. G., Pease, T. K., & Matsui, Y. (2010). Acquisition and assimilation of carbon in non-bleached and bleached corals. *Mar. Ecol. Prog. Ser.*, **420**, 91-101.

Hughes, A. D., & Grottoli, A. G. (2013). Heterotrophic compensation: a possible mechanism for resilience of coral reefs to global warming or a sign of prolonged stress? *PLoS ONE*, **8**, e81172.

Jeffery, S.W., and Humphrey, G.F. (1975) New spectrophotometric equations for determining chlorophylls a, b, c and c2 in higher plants, algae and natural phytoplankton. *Biochem. Physiol. Pflanz.* **167**, 191–194.

Johannes, R. E., Coles, S. L. and Kuenzel, N. T. (1970). The role of zooplankton in the nutrition of some scleractinian corals. *Limnol. Oceanogr*. **15**, 579–586

Johannes, R.E., Alberts, J., D'Elia, C., Kinzie, R.A., Pomeroy, L.R., Sottile, W., Wiebe, W., Marsh, J.A., Helfrich, P., Maragos, J., Meyer, J., Smith, S., Crabtree, D., Roth, A., McCloskey, L.R., Betzer, S., Marshall, N., Pilson, M.E.Q., Telek, G., Clutter, R.I., DuPaul, W.D., Webb K.L. and Wells, J. M. (1972) The metabolism of some coral reef communities: a team study of nutrient and energy flux at Eniwetok. *BioScience*, **22**, 541–543.

Kushmaro, A., & Kramarsky-Winter, E. (2004). Bacteria as a source of coral nutrition. In Coral Health and Disease (pp. 231-241). Springer Berlin Heidelberg.

Land, L. S., Lang, J. C., Smith, B. N. (1975) Preliminary observations on the carbon isotopic composition of some reef coral tissues and symbiotic zooxanthellae. *Limnol. Oceanogr.*, **20**, 283-287.

Leichter, J.J., Shellenbarger. G., Genovese, S.J. and Wing, S. R. (1998). Breaking internal waves on a Florida (USA) coral reef: a plankton pump at work? *Mar. Ecol. Prog. Ser.*, **166**, 83-97.

Lesser, M. P., Slattery, M., Stat, M., Ojimi M., Gates, R. D. and Grottoli, A. (2010) Photoacclimatization by the coral *Montastraea cavernosa* in the mesophotic zone: light, food, and genetics. *Ecology*, **91**, 990–1003.

Lester, N. P., Shuter, B. J. and Abrams, P. A. (2004) Interpreting the von Bertalanffy model of somatic growth in fishes: the cost of reproduction. *Proc. Roy. Soc. London B*, **271**, 1625-1631.

Leuzinger, S., Anthony, K. R. N. and Willis, B. L. (2003) Reproductive energy investment in corals: scaling with module size. *Oecologia* **136,** 524-561.

Marsh Jr, J. A. (1970). Primary productivity of reef-building calcareous red algae. *Ecology*, **51**, 255-263.

McCauley, E., Murdoch, W. W., Nisbet, R. M., Gurney, W. S. C. (1990) The physiological ecology of *Daphnia*: Development of a model of growth and reproduction. *Ecology*, **71**, 703-715

McKinnon, A. D., Richardson, A. J., Burford, M. A., and Furnas, M. J. (2007). Vulnerability of Great Barrier Reef plankton to climate change. In Climate Change and the Great Barrier Reef: A vulnerability assessment. Great Barrier Reef Marine Park Authority, Townsville.

Madin, J.S., Hoogenboom, M. O. and Connolly, S. R. (2012) Integrating physiological and biomechanical drivers of population growth over environmental gradients on coral reefs. *J. Exp. Biol.*, **215**, 968-976

Manzello, D. P. (2010) Coral growth with thermal stress and ocean acidification: lessons from the eastern tropical Pacific. *Coral Reefs*, **29**, 749–758.

Marshall, P. A. (2000) Skeletal damage in reef corals: relating resistance to colony morphology. *Mar. Ecol. Prog. Ser.*, **200**, 177-189.

Mills, M. M., Lipschultz, F. and Sebens, K. P. (2004). Particulate matter ingestion and associated nitrogen uptake by four species of scleractinian corals. *Coral Reefs* **23**, 311–323.

Muscatine, L. and Porter, J. W. (1977). Reef corals: mutualistic symbioses adapted to nutrient-poor environments? *BioScience* **27**, 454–459.

Muscatine, L. and Kaplan, I. R. (1994) Resource partitioning by reef corals as determined from stable isotope composition II. δ^{15}N of zooxanthellae and animal tissue versus depth. *Pac. Sci.* **48**, 304-312.

Muscatine, L., Porter, J. W. and Kaplan, I. R. (1989). Resource partitioning by reef corals as determined from stable isotope composition. I. δ13C of zooxanthellae and animal tissue vs depth. *Mar. Biol.*, **100**, 185–193.

Nahon, S., Richoux, N. B., Kolasinski, J., Desmalades, M., Pages, C. F., Lecellier, G., Planes, S., and Lecellier, V. B. (2013). Spatial and temporal variations in stable carbon (δ13C) and nitrogen (δ15N) isotopic composition of symbiotic scleractinian corals. *PLoS ONE*, **8**, e81247.

Odum, H. P. and Odum E. P. (1955) Trophic structure and productivity of a windward coral reef at Eniwetok Atoll, Marshall Islands. *Ecol. Monogr*., **25**, 291–320.

Palardy, J. E., Grottoli, A. G. and Matthews, K. A. (2005). Effects of upwelling, depth, morphology and polyp size on feeding in three species of Panamanian corals. *Mar. Ecol. Prog. Ser*. **300**, 79–89.

Palardy, J. E., Rodrigues, L. J., & Grottoli, A. G. (2008). The importance of zooplankton to the daily metabolic carbon requirements of healthy and bleached corals at two depths. *J. Exp. Mar. Biol. Ecol.*, **367**, 180-188.

Peterson, B. J., & Fry, B. (1987) Stable isotopes in ecosystem studies. *Ann. Rev. Ecol. Syst.*, **18**, 293-320.

Porter, J. W., Muscatine, L., Dubinsky, Z., & Falkowski, P. G. (1984). Primary production and photoadaptation in light-and shade-adapted colonies of the symbiotic coral, *Stylophora pistillata*. *Proc. Roy. Soc. London B*, **222**, 161-180.

Reynaud, S., Martinez, P., Houlbrèque, F., Billy, I., Allemand, D. and Ferrier-Pagès, C. (2009) Effect of light and feeding on the nitrogen isotopic composition of a zooxanthellate coral: role of nitrogen recycling. *Mar. Ecol. Prog. Ser*. **392**, 103-110.

Ribes, M., Coma, R., Atkinson, M. J., & Kinzie III, R. A. (2003). Particle removal by coral reef communities: picoplankton is a major source of nitrogen. *Mar. Ecol. Prog. Ser.*, **257**, 13-23.

Richardson, A. J. (2008). In hot water: zooplankton and climate change. *ICES J. Mar. Sci.*, **65**, 279-295.

Roder, C., Fillinger, L., Jantzen, C., Schmidt, G. M., Khokiattiwong, S., & Richter, C. (2010). Trophic response of corals to large amplitude internal waves. *Mar. Ecol. Prog. Ser.*, **412**, 113 - 128.

Saffo, M. B. (1992). Invertebrates in endosymbiotic associations. *Am. Zool*. **32**, 557–565.

Schiller, C., & Herndl, G. J. (1989). Evidence of enhanced microbial activity in the interstitial space of branched corals: possible implications for coral metabolism. *Coral Reefs*, **7**, 179-184.

Schneider, K., and Erez, J. (2006) The effect of carbonate chemistry on calcification and photosynthesis in the hermatypic coral *Acropora eurystoma*. *Limnol. Oceanogr.* **51**, 1284–1293.

Sebens, K. P. and Johnson, A. S. (1991) Effects of water movement on prey capture and distribution of reef corals. *Hydrobiologia*, **226**, 91–101.

Sebens, K. P., Vandersall, K. S., Savina, L. A., & Graham, K. R. (1996). Zooplankton capture by two scleractinian corals, *Madracis mirabilis* and *Montastrea cavernosa*, in a field enclosure. *Mar. Biol.*, **127**, 303-317.

Smith, S. V. (1981) The Houtman Abrolhos Islands carbon metabolism of coral reefs at high latitude. *Limnol. Oceanogr.*, **26**, 612-621

Swart, P. K. (1983). Carbon and oxygen isotope fractionation in scleractinian corals: a review. *Earth Sci. Rev.*, **19**, 51-80.

Tanaka, Y., Grottoli, A. G., Matsui, Y., Suzuki, A., & Sakai, K. (2015). Partitioning of nitrogen sources to algal endosymbionts of corals with long-term 15 N-labelling and a mixing model. *Ecol. Mod.*, **309**, 163-169.

Titlyanov, E.A, Tityanova, T. V., Yamazoto, K., and van Woesik, R. (2001) Photo-acclimation dynamics of the coral *Stylophora pistillata* to low and extremely low light. *J Exp. Mar. Biol. Ecol.*, **263**, 211-225.

Tremblay, P., Peirano, A. and Ferrier-Pages, C. (2011) Heterotrophy in the Mediterranean symbiotic coral *Cladocora caespitosa*: comparison with two other scleractinian species. *Mar. Ecol. Prog. Ser.* **422**, 167-177.

Tremblay, P., Grover, R., Maguer, J.F., Hoogenboom, M. and Ferrier-Pages, C. (2014) Carbon translocation from symbiont to host depends on irradiance and food availability in the tropical coral *Stylophora pistillata*. *Coral Reefs*, **433**, 1-13.

Tremblay, P., Maguer, J. F., Grover, R., & Ferrier-Pagès, C. (2015). Trophic dynamics of scleractinian corals: stable isotope evidence. *J. Exp. Biol.*, **218**, 1223-1234.

Weltzien F.-A., Hemre, G.I., Evjemo, J.O., Olsen, Y., and Fyhn, H.J. (2000) β-hydroxybutyrate in developing nauplii of brine shrimp (*Artemia franciscana* K.) under feeding and non-feeding conditions. *Comp. Biochem. Phys. B* **125**, 63–69.

Yahel, R., Yahel, G., Berman, T., Jaffe, J. S., & Genin, A. (2005). Diel pattern with abrupt crepuscular changes of zooplankton over a coral reef. *Limnol. Oceanogr.*, **50**, 930-944.

Yellowlees, D., Rees, T. W. and Leggatt, W. (2008). Metabolic interactions between algal symbionts and invertebrate hosts. *Plant Cell Env*. **31**, 679–694.

TABLES

Table 1: Mixed-effects analysis of variance of the effect of feeding on bioenergetics of five coral species, where ‘tank’ was included as a random effect. Non-significant interaction terms were removed from the analyses, data were square root or log transformed where required to enable the use of parameteric ANOVA.

Factor	**Df**	**F**	**p**
Symbiont density			
Species	4,46	72	<0.001
Feeding	1,4	47	<0.01
Species : Feeding	4,46	3.9	<0.01
Chlorophyll content			
Species	4,46	91	<0.001
Feeding	1,4	38	<0.01
Species : Feeding	4,46	3.7	<0.05
Photosynthesis rate			
Species	4,46	10.8	<0.001
Feeding	1,4	1.8	0.26
Species : Feeding	4,46	3.1	<0.05
Respiration rate			
Species	4,50	8.0	<0.001
Feeding	1,4	0.7	0.45
Protein content			
Species	4,50	58	<0.001
Feeding	1,4	21	<0.05
Lipid concentration			
Species	4,46	35	<0.001
Feeding	1,4	23	<0.01
Species : Feeding	4,46	4.0	<0.01
Calcification rate			
Species	4,50	29	<0.001
Feeding	1,4	4.4	0.11
Skeletal density			
Species	4,50	9.8	<0.001
Feeding	1,4	0.01	0.93
13c			
Species	4,20	8.5	<0.001
Feeding	1,20	16	< 0.001
Tissue	1,25	93	< 0.001
Species:Feeding	4,20	6.1	<0.01
Species:Tissue	4,25	9.2	<0.001
15N			
Species	2,11	55	<0.001
Feeding	1,11	52	<0.001
Tissue	1,12	0.17	0.69
Species:Tissue	2,12	4.7	<0.05

Table 2: Summary of the energy budget for fed corals of each of five species showing carbon intake from different sources.

Species	**Carbon budget**			
	Feeding Rate (nauplii cm^{-2} h^{-1})	Heterotrophic carbon intake relative to respiration (%)	Photosynthetic carbon intake relative to respiration (%)	Total carbon intake relative to respiration (%)
Acropora	9.6 (± 3.6)	19 (±6.8)	140 (±17.7)	160 (±14)
Galaxea	14.5 (± 2.1)	14 (±1.1)	141 (±7.7)	156 (±7.8)
Pocillopora	188 (± 15.9)	159 (±39)	106 (±13.4)	265 (±48)
Stylophora	103.8 (± 11.9)	75 (±8.8)	128 (±8.6)	203 (±16)
Turbinaria	50.3 (± 6.7)	36 (±3.8)	109 (±9.8)	145 (±13)

Table 3: Summary of the overall effects of heterotrophic feeding on physiological energetics for five coral species. '+' denotes a positive effect of feeding and '0' denotes no effect. Nd refers to 'no data' and 'host > sym' denotes difference between coral host and *Symbiodinium* regardless of feeding treatment. The 'feeding' main effect in Table 1 for $\delta^{15}N$ only applies to *Galaxea*, *Stylophora* and *Turbinaria* due to missing data for the tissue fraction of unfed colonies of *Acropora* and *Pocillopora*.

Effect of feeding on	**Species**				
	Acropora	*Galaxea*	*Pocillopora*	*Stylophora*	*Turbinaria*
Symbiont density	+	0	+	+	0
Chlorophyll content	+	0	0	0	+
Respiration rate	0	0	0	0	0
Photosynthesis rate	0	0	0	0	0
Calcification	0	0	0	0	0
Lipid content	0	0	+	0	+
Skeletal density	0	0	0	0	0
Protein content	+	+	+	+	+
Isotopic ratio					
$\delta^{15}N$	nd	+	Fed only, Host < Sym	+, Host > Sym.	+
$\delta^{13}C$	+, Host > Sym.	0, Host > Sym.	0, Host > Sym.	0	0

Table 4: Whole –community biomass and carbon uptake for simulated coral assemblages with a fixed horizontal planar area of 1.5 m^2. Values have been scaled up from measurements per unit surface area based on calculated colony tissue surface area per unit of horizontal area occupied as determined from colony morphology. For A) calculations were repeated using different morphologies for *Turbinaria*; conical refers to a cone-shaped colony with radius 25 cm and height 12 cm; multi-tier refers to a colony with two cone-shaped layers with radius 25 cm and height 12 cm and radius 15 cm and height 20 cm respectively. For B) calculations were repeated assuming different proportions of the tissue surface captured particulate matter.

Coral assemblage	Net carbon uptake (g C m^{-2} d^{-1})	Particulate carbon uptake (g C m^{-2} d^{-1})	Tissue biomass (g m^{-2})
A) *Galaxea*, *Turbinaria* (0.75 m^2 per genus)	0.66 – 0.87	0.25 – 0.63	24 - 33
with conical *Turbinaria*	0.66 – 0.87	0.25 – 0.63	24 - 33
with conical multi-tier *Turbinaria*	0.86 – 1.1	0.36 – 0.89	32 - 45
B) *Acropora*, *Stylophora*, *Pocillopora* (0.5 m^2 per genus)	9.9 – 12.9	7.2 - 10.5	139 - 206
Particle capture by 75% of polyps		5.4 – 7.9	
Particle capture by 50% of polyps		3.6 – 5.3	
Particle capture by 25% of polyps		1.8 – 2.6	
C) *Acropora*, *Stylophora*, *Pocillopora*, *Galaxea* & *Turbinaria* (0.3 m^2 per genus)	6.2 – 8.1	4.5 – 6.6	93 - 137

FIGURE LEGENDS

Fig 1: Effect of feeding on photosynthetic energy acquisition for five species of reef building corals. Error bars show standard deviation around mean values observed for each parameter and each species (n = 5 or 6), and points joined by dashed lines depict the magnitude of the feeding effect on symbiont density (‘Zoox’, panel A), chlorophyll concentration (‘Chl’, panel B), photosynthesis rate (‘Psyn’, panel C) and respiration rate (‘Resp’, panel D). Ns denotes a non-significant within-species feeding effect.

Fig 2: Effect of feeding on energy allocation to skeleton and tissue for five species of reef building corals. Error bars show standard deviation around mean values observed for each parameter and each species (n = 5 or 6), and points joined by dashed lines depict the magnitude of the feeding effect on total calcification measured using wet buoyant weight (A), protein and lipid content (B & C), and skeletal density (D). Ns denotes a non-significant within-species feeding effect and p-values reported for protein relates to the main-effect of feeding.

Fig 3. Effect of feeding on the nitrogen (A) and carbon (B) isotopic ratios for symbiont tissue (filled bars) versus host tissue (open bars) nubbins from five species of reef-building corals, differentiated by feeding regime (F = Fed, S = Unfed). Values are measured relative to isotopic composition of V-PDB for carbon and relative to air for nitrogen and the zero point is a relative rather than absolute measure.

Fig 4: Relationships between relative heterotrophic feeding capacity (CHAR) and A) energy allocation to tissue versus skeleton (%) for coral colonies; B) difference (‰) between host

and symbiont ^{13}C isotopic ratio: and C) difference (‰) between host and symbiont ^{15}N isotopic ratio. Only data for the fed colonies were included in the analyses (and plots) and error bars show standard error. P values in B and C indicate whether host and symbiont values different significantly within species, and S, T, A, P and G denote values for *Stylophora*, *Turbinaria*, *Acropora*, *Pocillopora* and *Galaxea* respectively. Values in B and C are measured relative to isotopic composition of V-PDB for carbon and relative to air for nitrogen and that the zero point is a relative rather than absolute measure.

Fig 5: Relationship between the difference between coral host and symbiont isotopic composition for carbon (x-axis) and nitrogen (y-axis) isotopes. Data points represent values for individual colonies for which both $\delta^{15}N$ and $\delta^{13}C$ data for both host and symbiont were obtained (N = 20). Both fed and unfed colonies of all 5 study species were included in this analysis.

Fig 6: Relationships between the symbiont density and the difference between coral host and symbiont isotopic composition for carbon (A) and nitrogen (B) isotopes. Data points represent values for individual colonies for which both $\delta^{15}N$ and $\delta^{13}C$ data for both host and symbiont were obtained. Both fed and unfed colonies of all 5 study species were included in this analysis. There are fewer data points in (B) due to missing data for δ15N for unfed colonies of *Acropora* and *Pocillopora*.

FIGURES

Fig 1

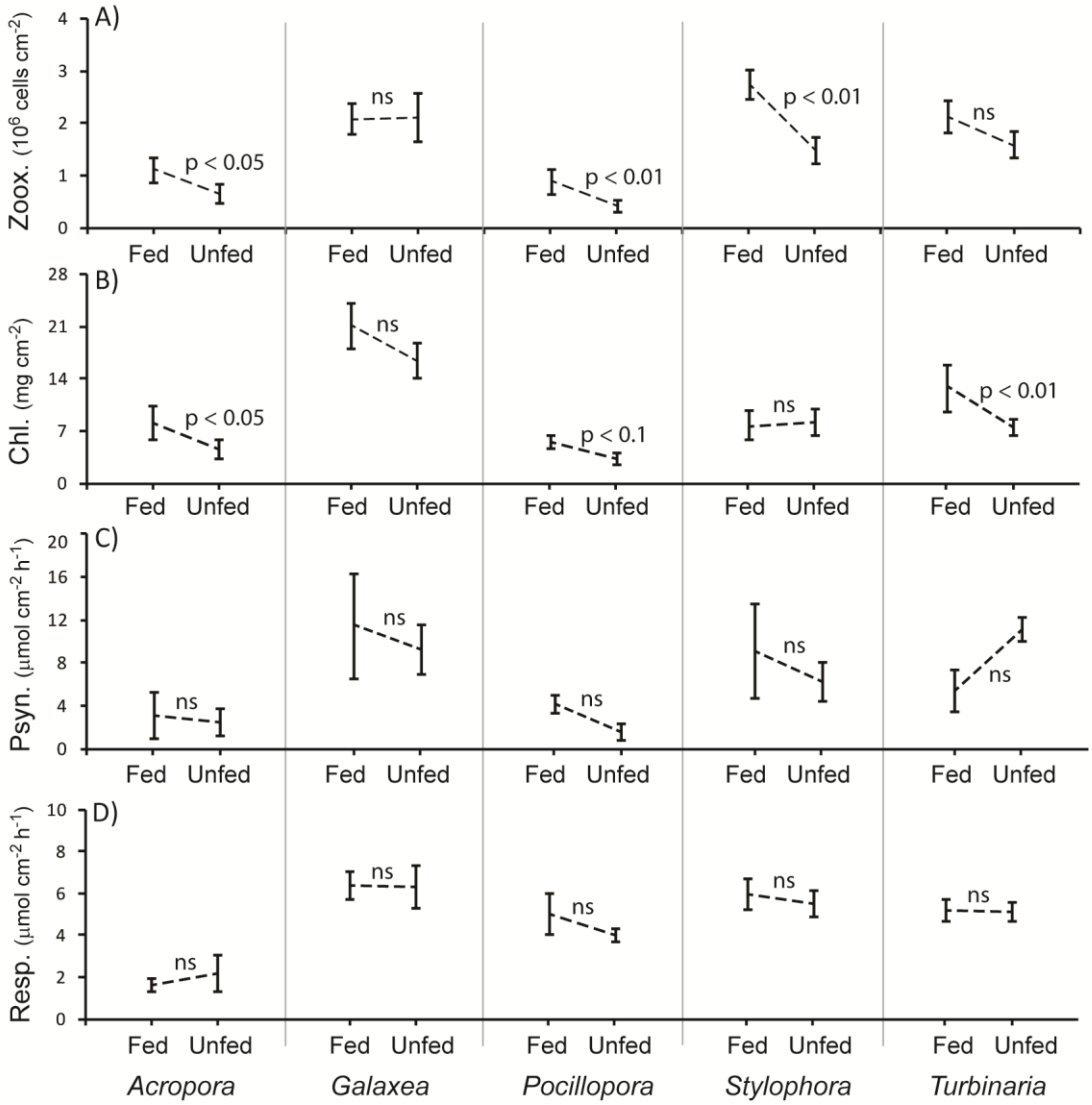

Fig 1: Effect of feeding on photosynthetic energy acquisition for five species of reef building corals. Error bars show standard deviation around mean values observed for each parameter and each species (n = 5 or 6), and points joined by dashed lines depict the magnitude of the feeding effect on symbiont density (‘Zoox’, panel A), chlorophyll concentration (‘Chl’, panel B), photosynthesis rate (‘Psyn’, panel C) and respiration rate (‘Resp’, panel D). Ns denotes a non-significant within-species feeding effect.

Fig 2

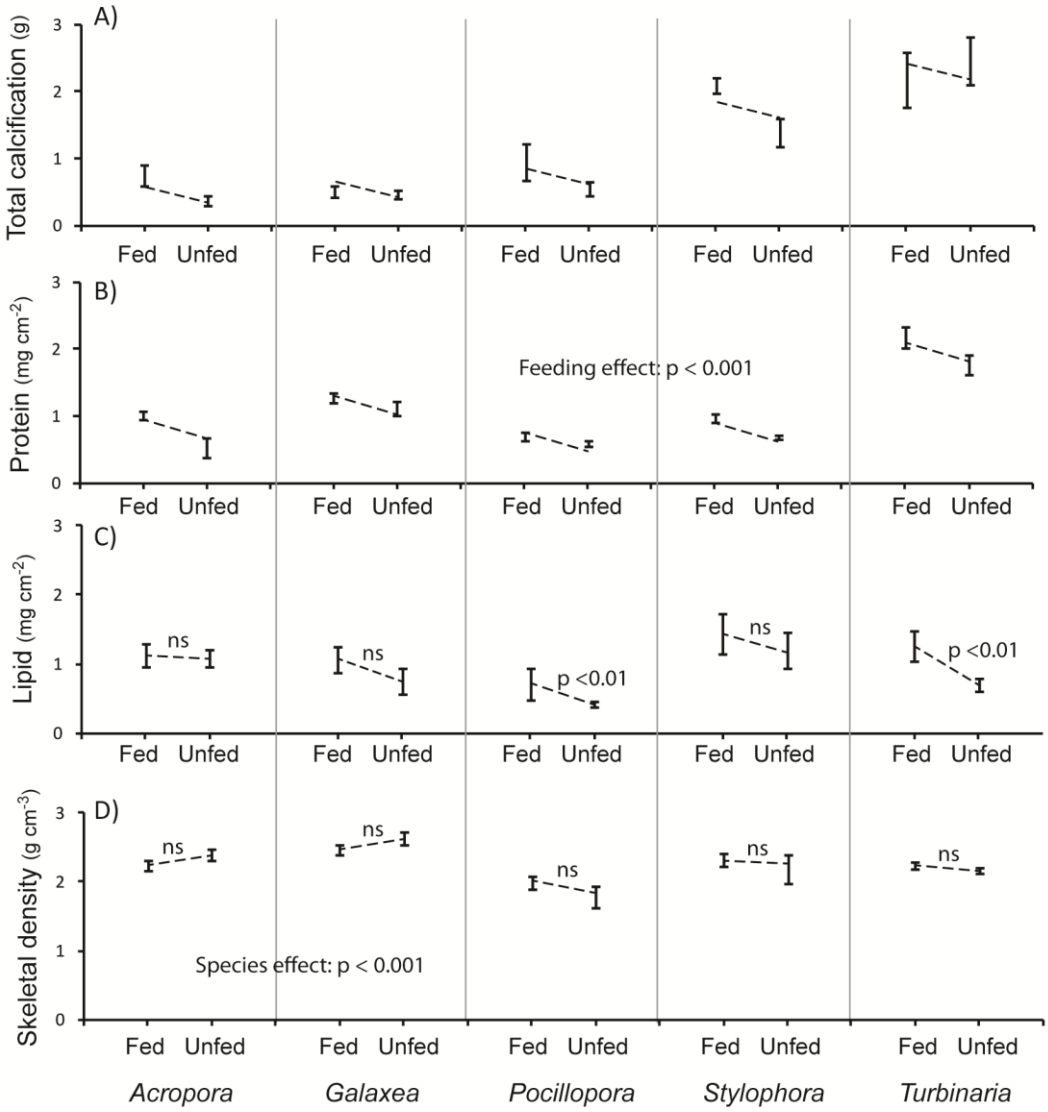

Fig 2: Effect of feeding on energy allocation to skeleton and tissue for five species of reef building corals. Error bars show standard deviation around mean values observed for each parameter and each species (n = 5 or 6), and points joined by dashed lines depict the magnitude of the feeding effect on total calcification measured using wet buoyant weight (A), protein and lipid content (B & C), and skeletal density (D). Ns denotes a non-significant within-species feeding effect and p-value reported for protein relates to the main-effect of feeding.

Fig 3

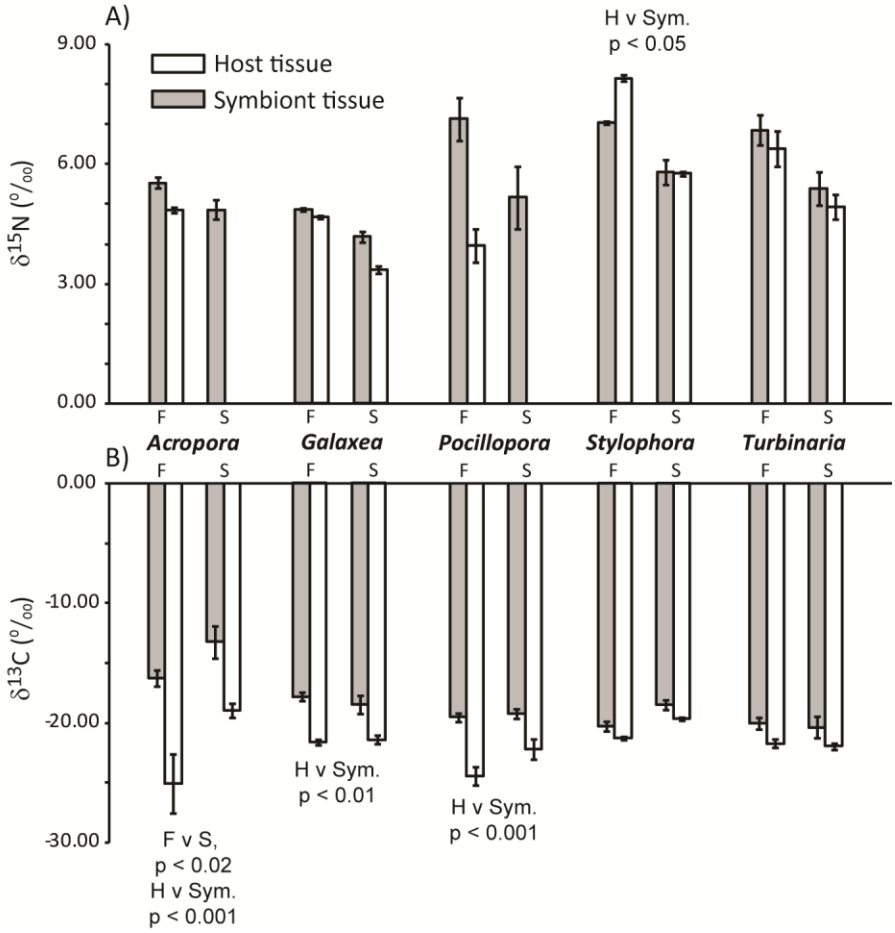

Fig 3. Effect of feeding on the nitrogen (A) and carbon (B) isotopic ratios for symbiont tissue (filled bars) versus host tissue (open bars) nubbins from five species of reef-building corals, differentiated by feeding regime (F = Fed, S = Unfed). Values are measured relative to isotopic composition of V-PDB for carbon and relative to air for nitrogen and the zero point is a relative rather than absolute measure.

Fig 4

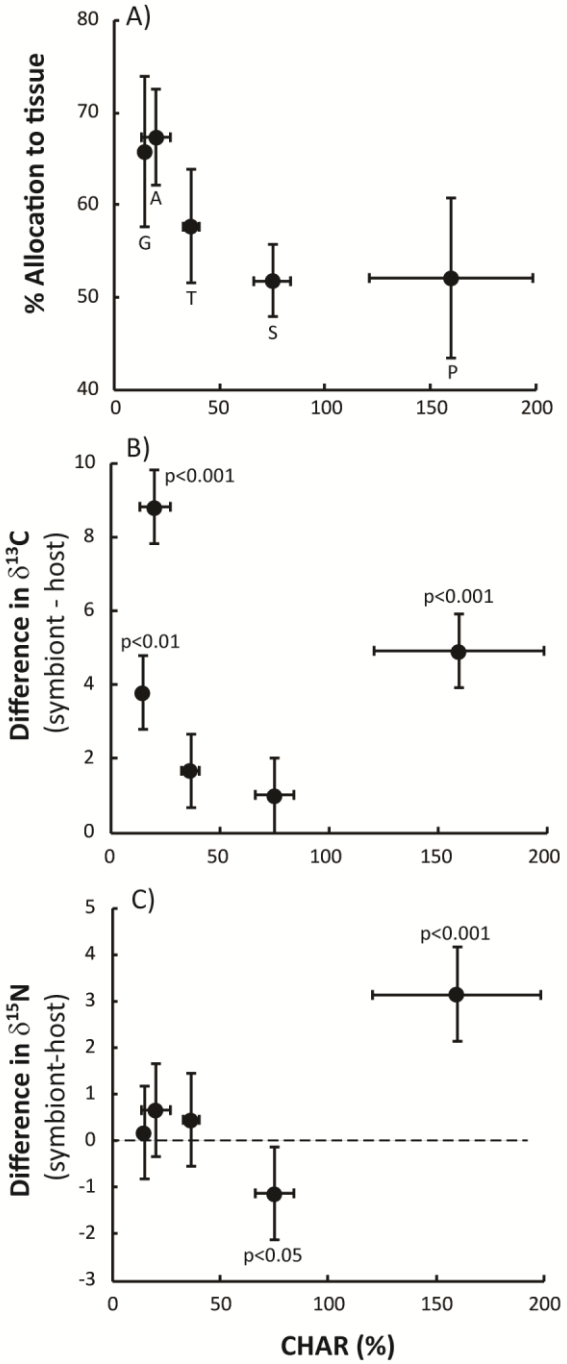

Fig 4: Relationships between relative heterotrophic feeding capacity (CHAR) and A) energy allocation to tissue versus skeleton (%) for coral colonies; B) difference (‰) between host and symbiont ^{13}C isotopic ratio: and C) difference (‰) between host and symbiont ^{15}N isotopic ratio. Only data for the fed colonies were included in the analyses (and plots) and error bars show standard error. P values in B and C indicate whether host and symbiont values different significantly within species, and S, T, A, P and G denote values for *Stylophora*, *Turbinaria*, *Acropora*, *Pocillopora* and *Galaxea* respectively. Values in B and C are measured relative to isotopic composition of V-PDB for carbon and relative to air for nitrogen and that the zero point is a relative rather than

absolute measure.

Fig 5

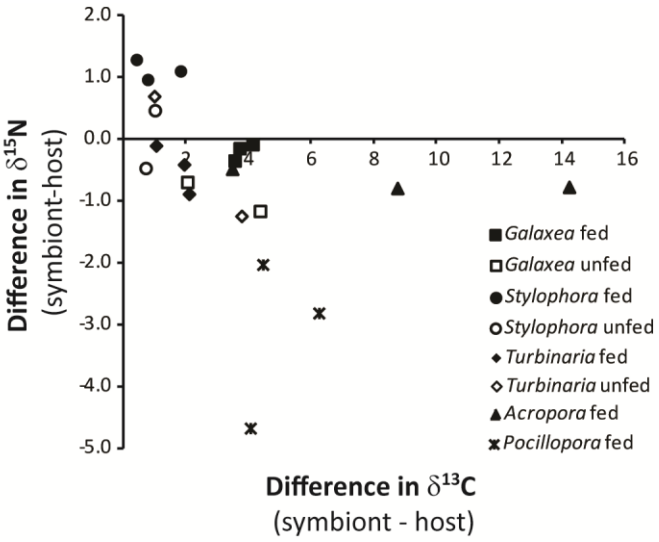

Fig 5: Relationship between the difference between coral host and symbiont isotopic composition for carbon (x-axis) and nitrogen (y-axis) isotopes. Data points represent values for individual colonies for which both $\delta^{15}N$ and $\delta^{13}C$ data for both host and symbiont were obtained (N = 20). Both fed and unfed colonies of all 5 study species were included in this analysis.

Fig 6

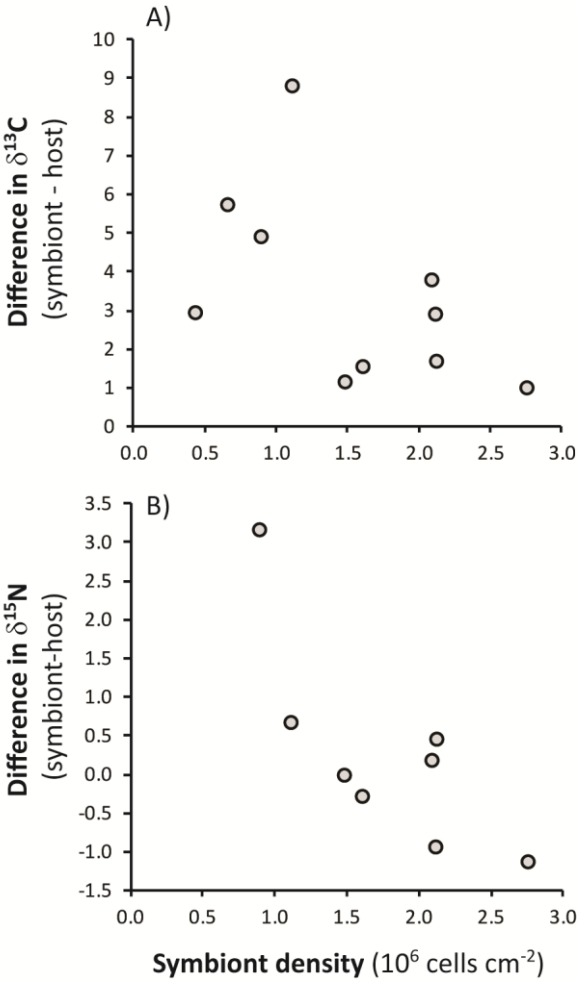

Fig 6: Relationships between the symbiont density and the difference between coral host and symbiont isotopic composition for carbon (A) and nitrogen (B) isotopes. Data points represent values for individual colonies for which both $\delta^{15}N$ and $\delta^{13}C$ data for both host and symbiont were obtained. Both fed and unfed colonies of all 5 study species were included in this analysis. There are fewer data points in (B) due to missing data for δ15N for unfed colonies of *Acropora* and *Pocillopora*.